



## THE NATURAL CONVECTION INSIDE A 3D TRIANGULAR CROSS SECTION CAVITY FILLED WITH NANOFLUID AND INCLUDED CYLINDER WITH DIFFERENT ARRANGEMENTS

Zainab Kareem GHOBEN <sup>1,2,\*</sup>, Ahmed Kadhim HUSSEIN <sup>2</sup>

<sup>1</sup> Ministry of Agriculture, Planning Department, Al-Diwaniya, Iraq

<sup>2</sup> University of Babylon, College of Engineering, Mechanical Engineering Department, Babylon City, Hilla, Iraq

\*Corresponding author, e-mail: [zainabghoben@gmail.com](mailto:zainabghoben@gmail.com)

### Abstract

In this paper the laminar unsteady natural convection heat transfer of (Al<sub>2</sub>O<sub>3</sub>-water) nanofluid inside 3D triangular cross section cavity was investigated. The cavity was heated differentially, the vertical walls were kept at different constant temperatures. The left hot and the right cold. The effect of the solid volume fraction was examined for two values and compared with the pure water results. The (Ra) range studied was (103 ≤ Ra ≤ 106). Inserting cylindrical body inside the cavity also investigated in three cases. One concentric cylinder has radius (15%) of the cavity side length. The other cases were of two cylinders having radius (7.5%) of the cavity side length, aligned vertically or nonaligned. The results show that the higher solid volume fraction gives the maximum enhancement of the average (Nu) and this enhancement increases with (Ra) increase. For the cases with inner cylinders, the average (Nu) enhanced for the case of double cylinders over single cylinder. On other hand, the nonaligned position of the cylinders giving more enhancement than other position. As like as, the location of maximum horizontal or vertical velocities were varied with the cylinders position while (Ra) has no effect.

Keywords: natural convection, triangular cavity, inner cylinder, nanofluid, 3D.

### Nomenclatures

$C_p$	Specific heat at constant pressure, J/Kg.K
$g$	Acceleration duo to gravity, m/s <sup>2</sup>
$K$	Thermal conductivity, W/m.K
$Nu$	Average Nusselt number
$P$	Pressure, N/m <sup>2</sup>
$Pr$	Prandtl number
$Ra$	Rayleigh number
$T$	Temperature, K
$t$	Time, s
$u$	The velocity component in x-direction, m/s
$v$	The velocity component in y-direction, m/s
$w$	The velocity component in z-direction, m/s
$x$	The coordinate in horizontal direction, m
$y$	The coordinate in vertical direction, m
$z$	The coordinate in axial direction, m

### Greek Symbols

$\alpha$	Thermal diffusivity, m <sup>2</sup> /s
$\beta$	Coefficient of thermal expansion, K <sup>-1</sup>
$\mu$	Dynamic viscosity, Kg/m.s
$\rho$	Density, Kg/m
$\phi$	Nanoparticles solid volume fraction

### Abbreviations

FE	Finite Element Method
M	
3D	Three-dimensional

### Subscribes

$c$	Cold
$eff$	Effective

$f$	Fluid
$h$	Hot
$nf$	Nano fluid
$p$	Solid particle

## 1. INTRODUCTION

A great attention was paid to the field of heat transfer by natural convection inside cavities due to the wide applications. Such as solar collector, nuclear reactors, passive cooling, lead-acid battery, geographical phenomena and double-pane window. Where this field was investigated numerically and experimentally in different simple or complex geometry of cavities [1-7]. The working fluids were classical fluids like air, water and other metals or using the nanofluids. Which is the suspicious of nanoparticles of metals or organic materials in classical fluids. These additives were improving the thermal properties of the fluid [8-10]. In this paper, the focusing will be applied to the 3D natural convection inside cavities numerically. Different researches were accomplished to study various parameters effect on the heat enhancement inside cavities. The parameters were the geometry of the cavity, the present of inner bodies inside these

cavities, the system of heating and cooling, the properties of the working fluids and etc.

For the natural convection inside simple classical cubical cavities filled with air, Li et al. [11] cavity having the opposite vertical walls were maintained at different temperatures. The other four walls were either adiabatic or have linear temperature variations or the front and back surfaces having linearly varied temperature. Kolsi et al. [12] used a cooler on the insulated bottom wall at the differentially heated cavity. The horizontal walls were adiabatic. Al-Rashed et al. [13] cavity was heated partially for different sidewall arrangements. A part of the left vertical sidewall was kept cold. A part of the opposite wall was kept hot. On the other hand, Gibanov and Sheremet [14-16] cavity equipped by a hot partition having triangular cross section. The vertical opposite walls were cooled while the rest walls were adiabatic [14]. After this, investigation of five various shapes of the heater cross section were performed [15]. Namely as rectangular, three trapezoidal and one triangular. At last, the team examined the variation of geometrical parameters of the trapezoidal heater (height, length, size) [16]. Spizzichino et al. [17] enclosure was cold including cold and hot vertically aligned cylinders. Alnaqi et al. [18] cavity with lateral active walls, the vertical front and right walls kept cold. While the vertical back and left were hot. While Fabregat and Pallares [19] cavity was heated by imposing a constant temperature at the bottom walls and cooled by imposing a constant temperature at the top walls. Another study by Alshomrani et al. [20] inside inclined cavity. On the left and right walls three unlike locations of the cooler were examined. Zemach et al. [21] immersed a horizontally aligned hot and cold cylinders inside a cold cavity. Also, filled with air, Hussein et al. [22] investigated an inclined trapezoidal cavity. The vertical right and left sidewalls were maintained cold. While the hot temperature was subjected to the lower wall.

For nanofluids natural convection inside classical cubical cavities, Kolsi et al. [23] studied the  $\text{Al}_2\text{O}_3$ -water in with left hot and right cold sidewalls of cavity. Kolsi et al. [24] cavity filled by  $\text{Al}_2\text{O}_3$ -water and containing twin adiabatic blocks. The vertical walls were differentially heated. Kolsi et al. [25] inserted solid baffle having triangular cross section at the corners of the cavity. Based on the number and location of these inserts, three cases were studied. At the same time, Kolsi et al. [26] inserted an adiabatic diamond shaped obstacle inside open cavities. For the same cavity shape, heating conditions and the nanofluid fills. Except that the liquid top surface was in contact with the gas Kolsi et al. [27] worked. Rahimi et al. [28] investigated the  $\text{CuO}$ -water nanofluid. The vertical walls of the cavity were heated differentially. Al-Rashed et al. [29] cavity was inclined filled by  $\text{CNT}$ -water and heated differentially. A conductive Ahmed body was centered inside the enclosure. Moutaouakil et al. [30] using three parallel heating elements on the left

vertical sidewall which had three inclinations. The cavity filled with ( $\text{Cu}$ ,  $\text{Al}_2\text{O}_3$ ,  $\text{Ag}$ ,  $\text{TiO}_2$ ) water based nanofluids. Sannad et al. [31-32] uses two different heat sources inside the cavity. The first was the partially heated left side wall [31] while the second was by using a hot partition [32]. In order to understand the effect of the ( $\text{Al}_2\text{O}_3$ ,  $\text{Cu}$  and  $\text{TiO}_2$ ) water based nanofluids. Esfe et al. [33] cavity equipped with different numbers of porous fins which filled with  $\text{CuO}$ -water and heated differentially. The cavity investigated by Selimefendigil and Oztop [34] was rectangular with one inclined side wall. Which having inner inclined T-shaped heat source. The inclined sidewall was kept at the higher temperature while the opposite vertical kept at the lower.

The non-classical shapes of cavities were also investigated. Where Al-Rashed et al. [35] cavity was parallelogrammatical filled with  $\text{CNT}$ -water. The vertical walls were differentially heated. Al-Rashed et al. [36] cavity was a parallelogrammatical opened top side, filled with  $\text{Al}_2\text{O}_3$ -water having heated square at the bottom side. While the remaining part of it was considered adiabatic. From other hand, Bendrer et al. [37] cavity was wavy cubical. The flow was partitioned into two layers; porous and hybrid nanofluid layers. The plans of the domain except upper and lower were kept at the low temperature. A rectangular heated area was located in the bottom plane.

From literature, it was clear that there were limited numerical studies on the not classical geometries of cavities especially the triangular shapes. But there were little numerical studies in two-dimensions like those of [38-42]. Where Xu et al. [38] cavity was triangular cold and tilted by different inclination angles and having inner hot cylinder. For a similar geometry, Yu et al. [39-40] studied the various ( $\text{Pr}$ ) values on the heat transfer [39]. Then, examined the unsteady natural convection [40]. Sourtihi et al. [41] cavity was like those of Xu et al. [38] but filled with nanofluid. While Amrani et al. [42] triangular cavity containing a rectangular obstacle. It was important to mention that; Kamiyo et al. [43] presented a comprehensive review on the natural convection in the triangular cavities. In this work, it was focused on the three dimensional differentially heated triangular side cross section cavity filled with nanofluid and included insulated cylinder in different arrangements. Where this configuration investigated for the first time.

The paper main object is to describe the flow and heat transfer fields inside the non-classical geometry cavity shape which is a triangular cross section. And the effect of inserting cylinder bodies inside the cavity on the heat transfer enhancement.

## 2. THE GEOMETRY

In this paper four cases for the triangular side cross section cavities were investigated as tabulated

in Table 1. One case without inner cylinders named Case1 and three cases with different conditions of inner cylinders as shown in Fig. 1. The first case was named Case2 with single cylinder having radius of about (15%) of the cavity side length while the two other cases having double cylinders of radius (7.5%) of the side length; named Case3 and Case4. Whereas Case3 cylinders was aligned while those of Case4 cylinders were nonaligned. The cavities were heated differentially, the left triangular wall was kept at the higher temperature. While the right was at the lower. The inner cylinders and all other walls were insulated. The working fluid for all the cases were the Al<sub>2</sub>O<sub>3</sub>-water nanofluid in two values of the solid volume fraction (0.02, 0.05). The properties of the (Al<sub>2</sub>O<sub>3</sub>) nano particles and the water base fluid were presented in Table 2. [44].

Table 1. The considered cases

The cavity	The inner cylinder	The cylinder radius (%) of cavity side length
Case1	-	-
Case2	Single concentric	15.0%
Case3	Double aligned	7.5%
Case4	Double non aligned	7.5%

Table 2. The physical properties [44]

	$\rho$ (Kg/m)	$C_p$ (J/Kg.K)	$K$ (W/m.K)	$\beta$ (K <sup>-1</sup> )
Pure Water	997.1	4179	0.613	0.0002100
Al <sub>2</sub> O <sub>3</sub>	3880	765	40	0.0000085

### 3. THE GOVERNING EQUATIONS

The assumptions below were chosen to describe the flow and heat transfer fields governing equations:

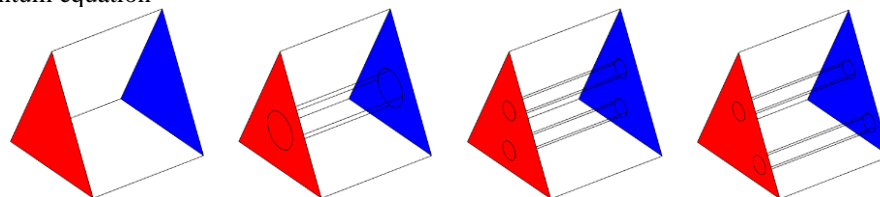
- Three-dimensional, time-dependent, incompressible and laminar flow.
- Radiation and heat generation are neglected.
- The base fluid and the nanoparticles are in thermal equilibrium.
- The fluid characteristics considered steady corresponding to Boussinesq approximation.

The FEM technique was employed to solve the governing equations numerically in the present work which were given as [32]:

The continuity equation

$$\frac{\partial u}{\partial x} + \frac{\partial v}{\partial y} + \frac{\partial w}{\partial z} = 0 \quad (1)$$

The momentum equation



(a) Case1. (b) Case2. (c) Case3. (d) Case4.

Fig. 1. The cavities configurations

In the x-direction:

$$\rho_{nf} \left( \frac{\partial u}{\partial t} + u \frac{\partial u}{\partial x} + v \frac{\partial u}{\partial y} + w \frac{\partial u}{\partial z} \right) = -\frac{\partial P}{\partial x} + \mu_{nf} \left( \frac{\partial^2 u}{\partial x^2} + \frac{\partial^2 u}{\partial y^2} + \frac{\partial^2 u}{\partial z^2} \right) \quad (2)$$

In the y-direction:

$$\rho_{nf} \left( \frac{\partial v}{\partial t} + u \frac{\partial v}{\partial x} + v \frac{\partial v}{\partial y} + w \frac{\partial v}{\partial z} \right) = -\frac{\partial P}{\partial y} + \mu_{nf} \left( \frac{\partial^2 v}{\partial x^2} + \frac{\partial^2 v}{\partial y^2} + \frac{\partial^2 v}{\partial z^2} \right) - \rho_{nf} g \quad (3)$$

In the z-direction:

$$\rho_{nf} \left( \frac{\partial w}{\partial t} + u \frac{\partial w}{\partial x} + v \frac{\partial w}{\partial y} + w \frac{\partial w}{\partial z} \right) = -\frac{\partial P}{\partial z} + \mu_{nf} \left( \frac{\partial^2 w}{\partial x^2} + \frac{\partial^2 w}{\partial y^2} + \frac{\partial^2 w}{\partial z^2} \right) \quad (4)$$

The energy equation

$$\frac{\partial T}{\partial t} + u \frac{\partial T}{\partial x} + v \frac{\partial T}{\partial y} + w \frac{\partial T}{\partial z} = \alpha_{nf} \left( \frac{\partial^2 T}{\partial x^2} + \frac{\partial^2 T}{\partial y^2} + \frac{\partial^2 T}{\partial z^2} \right) \quad (5)$$

The average Nusselt number equation.

The (Nu) was presented as [9]:

$$Nu = \int_0^1 \int_0^1 (Nu) dy dz \quad (6)$$

The nanofluid properties equations were represented by appropriate models which are given by [45,46]:

The thermal diffusivity

$$\alpha_{nf} = \frac{K_{nf}}{(\rho c_p)_{nf}} \quad (7)$$

The dynamic viscosity

$$\mu_{nf} = \frac{\mu_f}{(1-\phi)^{2.5}} \quad (8)$$

The effective density

$$\rho_{nf} = (1 - \phi)\rho_f + \phi\rho_p \quad (9)$$

The heat capacitance

$$(\rho c_p)_{nf} = (1 - \phi)(\rho c_p)_f + \phi(\rho c_p)_p \quad (10)$$

The model of Maxwell–Garnetts was used to describe the effective thermal conductivity of nanofluid, which was approximated for spherical nanoparticles:

$$K_{eff} = \frac{K_{nf}}{K_f} = \frac{(K_p + 2K_f) - 2\phi(K_f - K_p)}{(K_p + 2K_f) + \phi(K_f - K_p)} \quad (11)$$

The previous equations were solved using the following boundary conditions and initial conditions as shown in Fig. (2):

1. The left sidewall maintained at hot temperature:  
At  $x=0, T=T_h, u=v=w=0$
2. The right sidewall maintained at cold temperature:  
At  $x=L, T=T_c, u=v=w=0$
3. The remained walls and the inner cylinders are kept insulated:

$$\frac{\partial T}{\partial x} = \frac{\partial T}{\partial y} = \frac{\partial T}{\partial z} = 0, u=v=w=0$$

The fluid domain initial condition was:

$$T = \frac{T_h + T_c}{2}$$

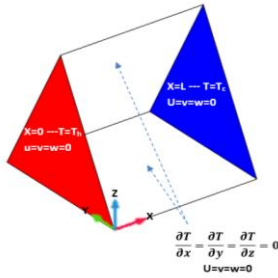


Fig. 2. The boundary conditions

#### 4. THE NUMERICAL METHODOLOGY

The FEM were used to solve the governing equations of the fluid flow and the unsteady laminar natural convection heat transfer of the nanofluid inside the described cavities. The grid independence test was examined for all the four cases according to the stability of the (Nu) value. For Case1 the grid independence procedure was introduced in Table 3. Taking into account the time consumed comparing to the error when choosing the suitable mesh. While the selected mesh for all the cases were presented in Table 4. and Fig. 3. On the other hand, the validation of this study was approved by satisfying the results of the previous studies and getting a very close results with them as presented in Table 5. Also, the results for the stream lines and the isotherm lines configurations were validated with that performed by Sannad et al. [31] at ( $Ra = 10^4$  and  $\phi = 0.04$ ) as presented in Fig. 4.

Table 3. The grid independence test according to Nu stability at  $Ra = 10^4$  and  $\phi = 0.05$  for Case1

Domain elements	Boundary elements	Edges elements	Nu	Time (sec)
9829	1836	143	1.6461	128
29607	3244	179	1.6610	315
38516	4946	259	1.6666	523
63826	5874	259	1.6714	1078
93578	9988	416	1.6736	1171
198837	13300	416	1.6733	2079

Table 4. The selected grid for each case

Cases	Domain elements	Boundary elements	Edges elements
Case1	093578	09988	416
Case2	166003	14238	680
Case3	190352	15490	864
Case4	188508	15584	864

Table 5. The Nu verification with previous published data

Author	$Ra = 10^4$	$Ra = 10^5$
Tric [47]	2.2450	4.5220
Peng [48]	2.3040	4.6580
Purusothaman [49]	2.2558	4.6269
Present	2.2548	4.5997

#### 5. RESULTS AND DISCUSSION

The three-dimensional natural convection inside a triangular side cross section cavity filled with ( $Al_2O_3$ -water) nanofluid was performed. The effect of the solid volume fraction ( $\phi$ ) of the nanoparticles and ( $Ra$ ) on the fluid flow and the heat transfer fields were discovered in the following sections. In order to get better view of the 3D results, three different

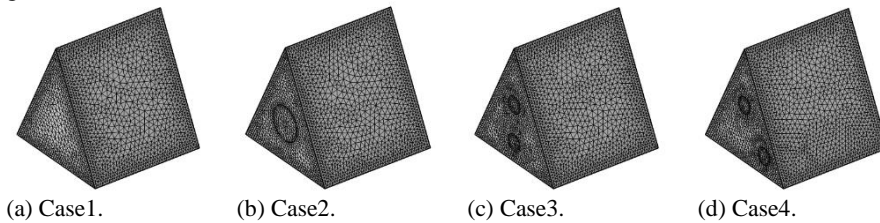


Fig. 3. The selected mesh for the different cases

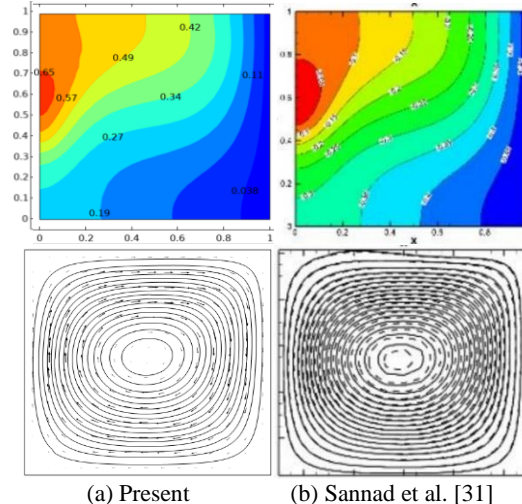


Fig. 4. The validation of the present data with Sannad et al. [31], isotherms (up) and streamlines (down)

planes were considered. Which was located laterally between the hot and cold walls of the cavity which were parallel to the (X-Z) plane. These surfaces were positioned perpendicular to the bottom wall and chosen at ( $Y= 1/2, 1/4, 3/4$ ) which named (P1, P2, P3) respectively as Fig. 5 shows. The choice of these planes because that the plane (P1) located at the middle of the cavity and it was the highest. While (P2) and (P3) viewing the similarity or non-similarity of the inner domain and it crosses the inner bodies in the cases (Case2, Case3, Case4).

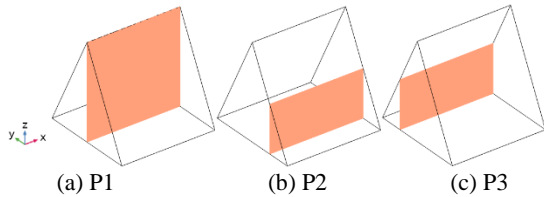


Fig. 5. The selected data planes

**5.1. Cavity without inner cylinder**

**5.1.1. The flow structure**

The three-dimensional flow structure of natural convection inside a triangular side cross section at ( $Ra=10^5$  and  $\phi=0, 0.02, 0.05$ ) was presented in Fig. 6 below. The figure presents the effect of nanoparticles loading on the pure water flow structure. First of all, it was important to say that the flow for all working fluids conditions that the flow was identical around (P1). By means of similar flow behavior in front and behind of it. For all the states

the flow appears in single clockwise circulation configuration. The circulated flow of the particles inside the cavity clockwise horizontally along the (X-axis) then vertically along (Z-axis) from the hot to the cold sidewall. For pure water ( $\phi=0$ ) the core of the flow circulation was circular while for the nanofluid states ( $\phi=0.02$  and  $0.05$ ) its shape was an elongated ellipse. Also, it was observed for nanofluid states that the streamlines closer to each other near the cavity walls while it was far from each other with closing to the center of the cavity. For state of water, these lines were nearly uniform in distribution. From the other hand, the (Ra) effect on the working fluid flow streamlines was presented on (P1) in Fig. 7 to discover the effect of different ( $Ra = 10^3, 10^4, 10^6$ ). For ( $Ra=10^3$ ) all the states of water or nanofluid with different solid volume fraction ( $\phi=0.02$  and  $0.05$ ), the core of the circulation flow was circular. For nanofluid, by increasing (Ra) the core hole begin to elongate to form shape closer to elliptical shape and enlarged in size till its bounded nearly touch the walls of the cavity. Making the region of stagnant fluid become wide. While for water the shape of the flow streamlines still the same or its change was insignificant. From the Figs. 6 and 7, another important observation was that the streamlines shape insignificant to the solid volume fraction variation. But the value of maximum magnitude of the horizontal velocity (u) and the vertical velocity (w) were affected. Which entirely increases with the solid volume fraction increase.

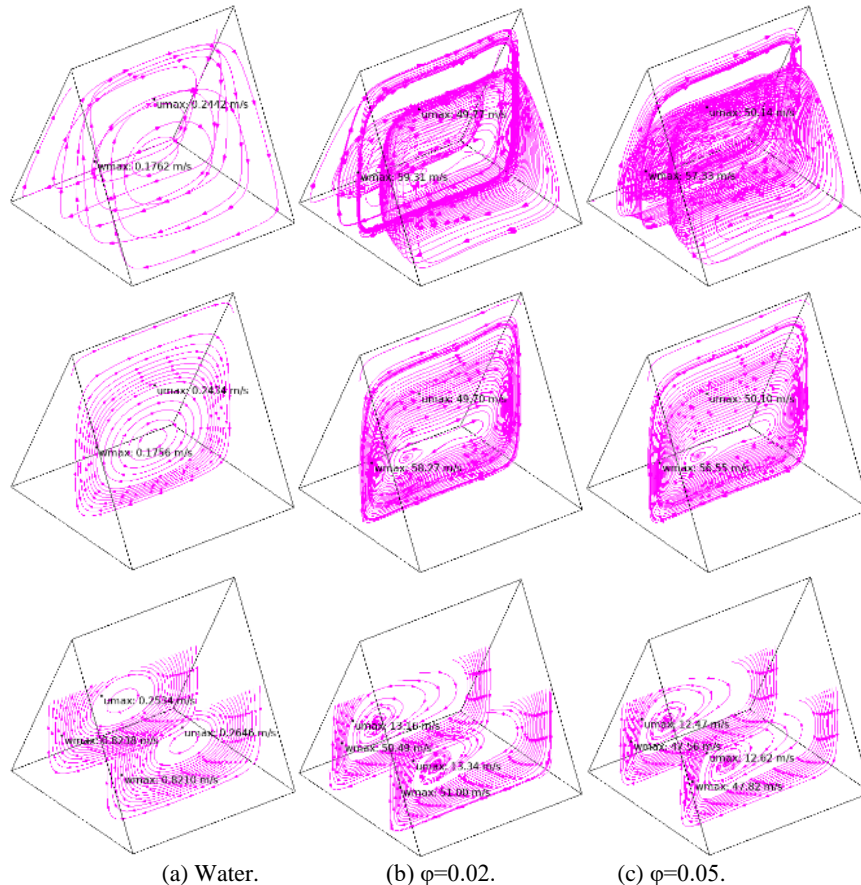


Fig. 6. The streamlines of Case1 at  $Ra=10^5$

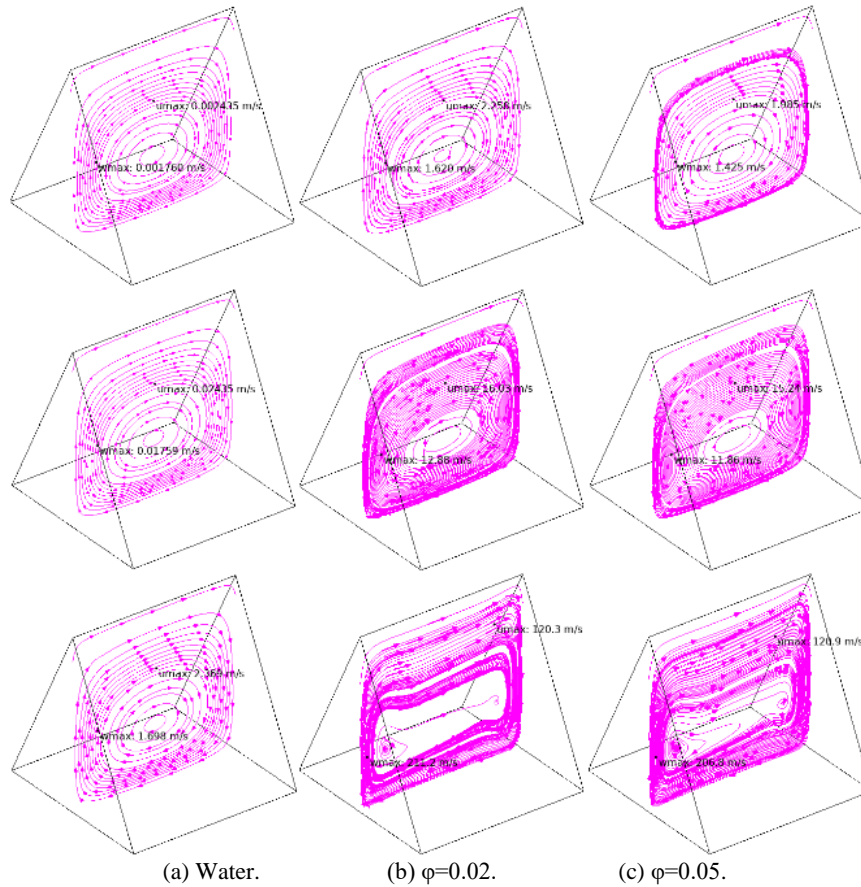


Fig. 7. The streamlines of Case1 at  $Ra$  ( $10^3, 10^4, 10^6$ ) (up to down)

For more explanations, Fig. 8 presented the maximum values of ( $u$ ) and ( $w$ ) for the three working fluid states versus ( $Ra$ ). For water working fluid, both ( $u$ ) and ( $w$ ) increases with ( $Ra$ ) increase and always ( $u$ ) was higher than ( $w$ ). For nanofluid working fluid as like as water, both ( $u$ ) and ( $w$ ) increase with increase of ( $Ra$ ). But for ( $Ra < 4.6 \times 10^4$ ) ( $u$ ) was higher than ( $w$ ) for all cases. The inverse behavior occurs at ( $Ra > 4.6 \times 10^4$ ) where ( $u$ ) becomes lower than ( $w$ ) for all cases also. Likely, for all ( $Ra$ ) range both ( $u$ ) and ( $w$ ) for state ( $\phi=0.02$ ) was higher than that of ( $\phi=0.05$ ). Which explaining the decelerating of the flow of particles with increasing the solid volume fraction.

### 5.1.2. The heat transfer

The temperature iso-surfaces for the different working fluid states: water, nanofluid ( $\phi=0.02$  and  $0.05$ ) versus the range of ( $Ra$ ) were presented in Fig. 9 below. For water, the variation of ( $Ra$ ) was not affect the isotherm lines which still uniform for the range ( $10^3 \leq Ra \leq 10^5$ ). For ( $Ra=10^6$ ) a slight ripple appears on these lines, but still in harmonious and parallel to the cavity vertical walls. For the nanofluid states; the uniformity of the streamlines was affected strongly by increasing ( $Ra$ ). On the other hand, no effect of the solid volume fraction on the isotherm lines configuration inside cavities were observed. The nonuniformity of the isotherm lines of the nanofluid states was clear explaining the convection dominant heat transfer while those of water state

meaning no convection accelerated yet although of the value of ( $Ra$ ). As like as streamlines, the isotherm lines were identical around ( $P1$ ) were the behavior in front of it exactly similar to that behind it as presented in Fig. 10. Dislike the isotherm lines behavior; a great effect of the solid volume fraction on ( $Nu$ ) was appointed. It was noticed that the ( $Nu$ ) increases significantly when comparing nanofluid to the pure water as shown in Fig. 11. And for nanofluid ( $Nu$ ) increased by the solid volume fraction increase. This increase in ( $Nu$ ) was higher at ( $Ra=10^3$  and  $10^6$ ) while it was lower at other ( $Ra$ ). As well as; by increasing ( $Ra$ ) ( $Nu$ ) increase for both classical and nanofluid by increasing ( $Ra$ ).

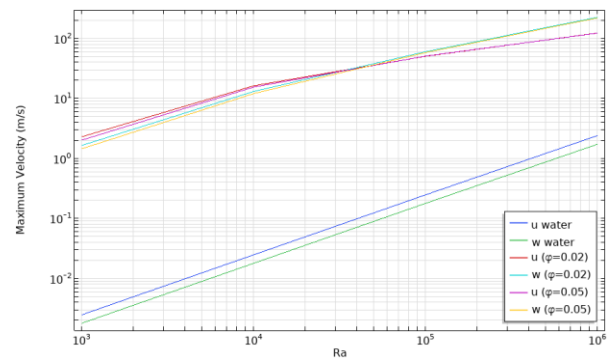


Fig. 8. The maximum velocity versus  $Ra$  for Case1



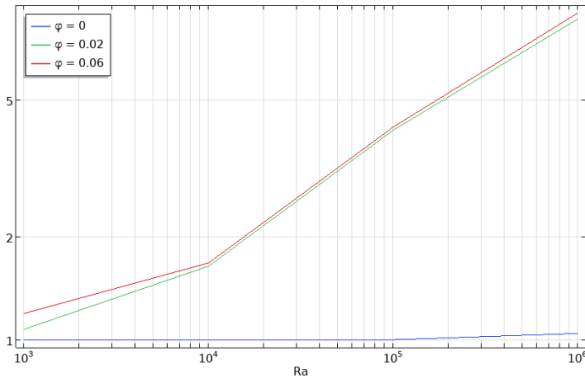


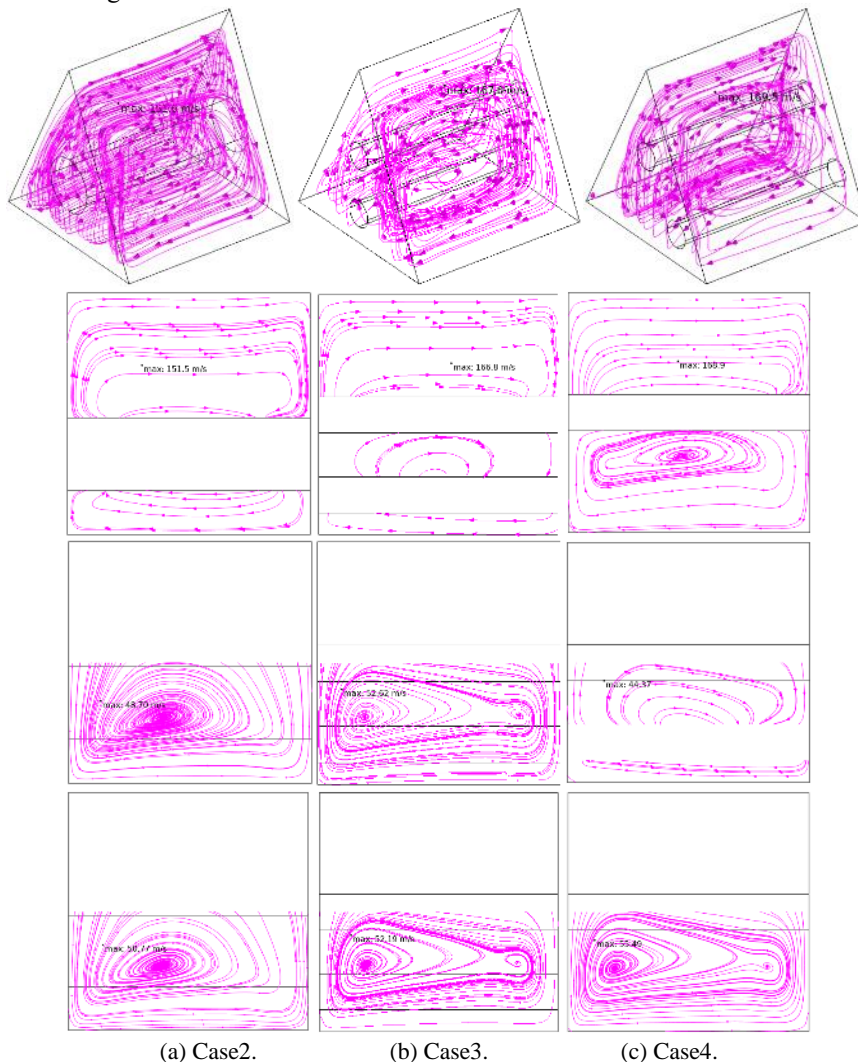
Fig. 11. The Nu versus Ra for Case1

## 5.2. Cavities with inner cylinders

### 5.2.1. The flow structure

The flow structure in three-dimensional (the streamlines) inside the cavity at ( $\varphi=0.05$ ) and ( $Ra=10^6$ ) as like as two-dimensional on the selected data planes (P1, P2, P3) for all cases were presented in Fig. 12 below. As it shown that there was two main clockwise circulation for the Case1 and Case3. Which was located above and below the inner cylinders. While it was three circulations for Case2 above, below and between the inner cylinders because that it was aligned to each other. It's

important to mention that; the inner cylinders change the streamlines profile. The core of the single vortex on (P1) was pushed down when there is an inner cylinder crossing it which tending to make more than one vertex. Also, it was observed that the Case1 and Case2 were identical respect to (P2) and (P3). While Case3 was of different flow structure on these planes. On (P2) and (P3) the circulation of Case1 has one nearly circular core located at the half of cavity which was closer to the hot sidewall. For Case2 the circulation taking an elongated elliptical shape with two cores, the larger closer to the hot sidewall and the smaller closer to the cold sidewall. The circulated flow of the particles inside the cavity clockwise horizontally along the (X-axis) then vertically along (Z-axis) from the hot to the cold sidewall. The maximum magnitude of the horizontal and vertical velocities ( $u$ ) and ( $w$ ) with respect to ( $Ra$ ) at ( $\varphi=0.05$ ) were presented in Fig. 13. For ( $Ra < 4.6 \times 10^4$ ) the horizontal velocity ( $u$ ) was higher than the vertical ( $w$ ) for all cases. The inverse behaviour occurs at ( $Ra > 4.6 \times 10^4$ ) where ( $u$ ) becomes lower than ( $w$ ) for all cases also. For all ( $Ra$ ) range, the maximum value of ( $u$ ) was arranged from higher to lower as (Case3, Case2, Case1) respectively. While it was (Case1, Case3, Case2) in turn for ( $w$ ).

Fig. 12. The streamlines at  $Ra=10^6$  and  $\varphi=0.05$

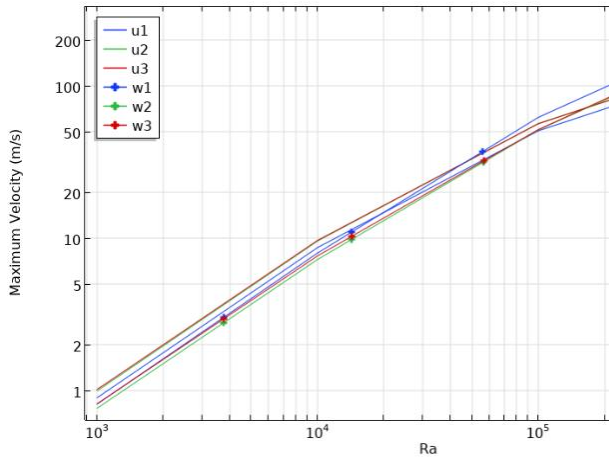


Fig. 13. The maximum velocities for all cases versus Ra at  $\phi=0.05$

**5.2.2. The heat transfer**

The iso-surfaces of the cases with inner cylinders were presented in Fig. 14 at  $(Ra=10^6)$  and  $(\phi=0.05)$ . The inner cylinders increase the nonlinearity of these lines, meaning that accelerating the convection appearance. This nonlinearity increased in the cases with two cylinders causing more enhancement in the heat transferred through the cavity. The Figs. 15 and 16 represent the isotherm lines on the (P1), (P2) and (P3) as like as streamlines, the Case4 was non-identical in isotherm lines on (P2) and (P3) duo to

the non-identical location of the inner cylinders' location. The Fig. 17 represents the  $(Nu)$  versus the  $(Ra)$  for the cases with inner cylinders. The double inner cylinders cavities have higher values of the  $(Nu)$  than that of single inner cylinder. And the non-aligned cylinders case has higher than that of the case of aligned cylinders. This difference or increase in  $(Nu)$  value of Case4 over Case3 reaching its peak value at  $(Ra=10^5)$  while this increase disappeared at  $(Ra=10^3)$  and  $(Ra=10^6)$ .

**6. CONCLUSIONS**

The unsteady natural convection heat transfer inside triangular cross-sectional cavity was studied in four cases, one without inner cylinder named Case1 and three cases with inner cylinders. One of these three cases which named Case2 having single inner cylinder, the Case3 having double aligned inner cylinders. While Case4 having double non-aligned inner cylinders. Some concluding observations from the investigation are given below.

- For the nanofluid states the streamlines shape insignificant to the solid volume fraction variation while it was affected by changing  $(Ra)$  as like as for the water working fluid state. Whereas the maximum  $(u)$  and  $(w)$  increases with the solid volume fraction increase.

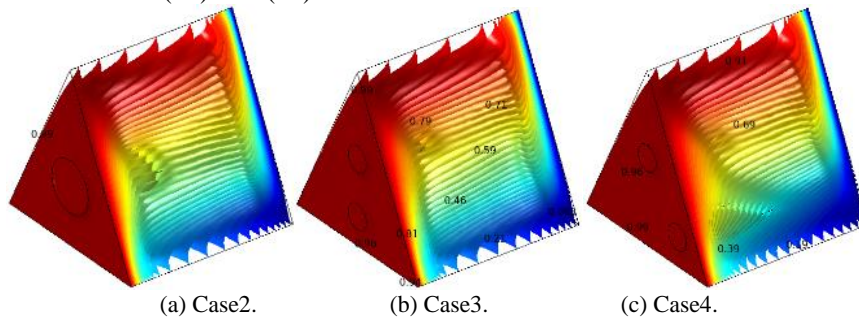


Fig. 14. The temperature iso-surfaces at  $Ra=10^6$  and  $\phi=0.05$

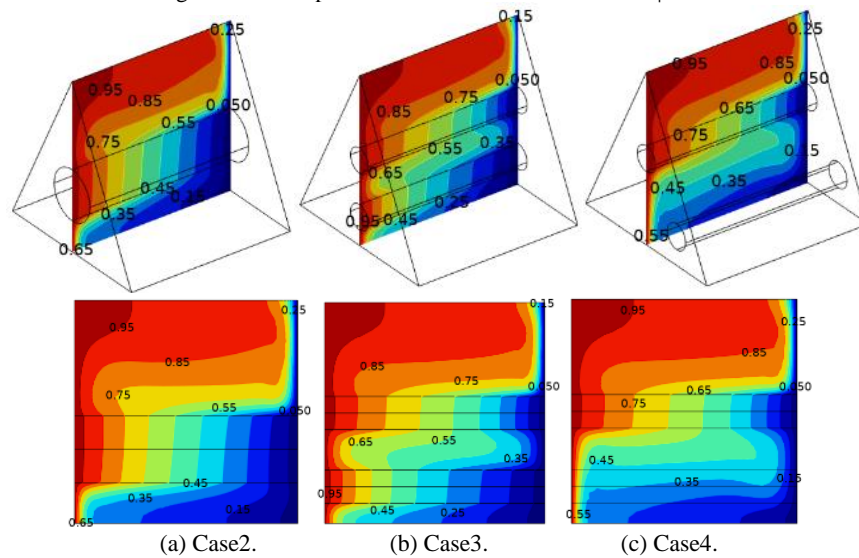


Fig. 15. The temperature isotherm lines at  $Ra=10^6$  and  $\phi=0.05$

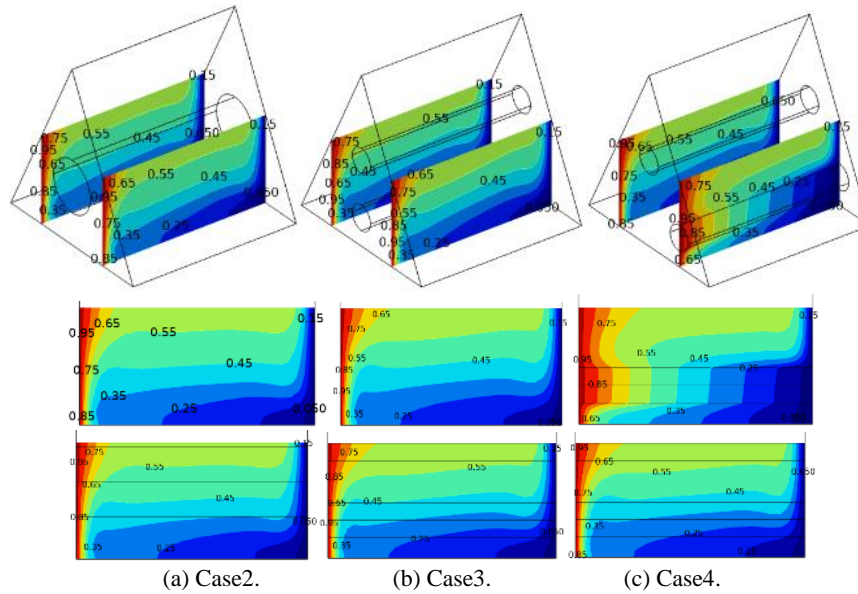


Fig. 16. The isotherm lines at  $Ra=10^6$  and  $\phi=0.05$ .

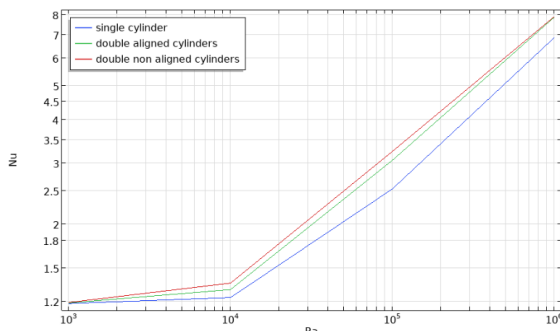


Fig. 17. The Nu versus Ra at  $\phi=0.05$

- Also, the solid volume fraction has no effect on the isotherm lines configuration inside cavities. But, the (Nu) increases when comparing nanofluid to the pure water and (Nu) increased by the solid volume fraction increase.
- The (Nu) increase for both classical and nanofluid by increasing (Ra). And this increase was higher at ( $Ra=10^3$  and  $10^6$ ) while it was lower at other (Ra) values.
- The including of inner cylinders changing the streamlines profile. Where the nonlinearity increased in the cases with two cylinders causing more enhancement in the heat transferred through the cavity.
- For all (Ra) range, the maximum (u) was arranged from higher to lower as (Case3, Case2, Case1). While for (w) it was (Case1, Case3, Case2).
- The non-aligned cylinders case (Case4) has higher than that of the case of aligned cylinders (Case3).
- The increase in (Nu) value of (Case4) over (Case3) reaching its peak value at ( $Ra=10^5$ ) while this increase disappeared at ( $Ra=10^3$ ) and ( $Ra=10^6$ ).

**Author contributions:** research concept and design, Z.K.G., A.K.H.; Collection and/or assembly of data, Z.K.G.; Data analysis and interpretation, Z.K.G.; Writing the article, Z.K.G.; Critical revision of the article, Z.K.G., A.K.H.; Final approval of the article, Z.K.G., A.K.H.

**Declaration of competing interest:** The authors declare that they have no known competing financial interests or personal relationships that could have appeared to influence the work reported in this paper.

## REFERENCES

1. Baïri A, Zarco-Pernia E, García de María JM. A review on natural convection in enclosures for engineering applications. The particular case of the parallelogrammic diode cavity Applied Thermal Engineering. 2014;63:304-322. <http://dx.doi.org/10.1016/j.applthermaleng.2013.10.065>.
2. Ayed SK, Al Guboori AR, Hussain HM, Habeeb LJ. Review on enhancement of natural convection heat transfer inside enclosure. Journal of Mechanical Engineering Research and Developments. 2021;44 (1):123-134.
3. Rostami S, Aghakhani S, Pordanjani AH, Afrand M, Cheraghian G, Oztop HF, Shadloo MS. A review on the control parameters of natural convection in different shaped cavities with and without nanofluid. Processes. 2020;8(9). <https://doi.org/10.3390/pr8091011>
4. Giwa SO, Sharifpur M, Ahmadi MH, Meyer JP. A review of magnetic field influence on natural convection heat transfer performance of nanofluids in square cavities. Journal of Thermal Analysis and Calorimetry. 2020;145:2581–2623 <https://doi.org/10.1007/s10973-020-09832-3>
5. Öztop HF, Estellé P, Yan WM, Al-Salem K, Orfi J, Mahian O. A brief review of natural convection in enclosures under localized heating with and without nanofluids International Communications in Heat and Mass Transfer. 2015;60:37-44 <http://dx.doi.org/10.1016/j.icheatmasstransfer.2014.11.001>.

6. Hussein AK, Awad MM, Kolsi L, Fathinia F, Adegun IK. A comprehensive review of transient natural convection flow in enclosures. *Journal of Basic and Applied Scientific Research*, 2014;4 (11):17-27.
7. Das D, Roy M, Basak T. Studies on natural convection within enclosures of various (non-square) shapes – A review. *International Journal of Heat and Mass Transfer*, 2017;106:356–406. <http://dx.doi.org/10.1016/j.ijheatmasstransfer.2016.08.034>.
8. Kolsi L, Lajnef E, Aich W, Alghamdi A, Aichouni MA, Borjini MN, Aïssia HB. Numerical investigation of combined buoyancy-thermocapillary convection and entropy generation in 3D cavity filled with Al<sub>2</sub>O<sub>3</sub> nanofluid”, *Alexandria Engineering Journal*. 2016;56(1):71-79. <http://dx.doi.org/10.1016/j.aej.2016.09.005>.
9. Rahimi A, Kasaeipoor A, Malekshah EH, Rashidi MM, Purusothaman A. Lattice Boltzmann simulation of 3D natural convection in a cuboid filled with KKL-model predicted nanofluid using Dual-MRT model. *International Journal of Numerical Methods for Heat and Fluid Flow*. 2018; 29(1):365-38 <https://doi.org/10.1108/HFF-07-2017-0262>.
10. Esfe MH, Barzegarian R, Bahiraei M. A 3D numerical study on natural convection flow of nanofluid inside a cubical cavity equipped with porous fins using two-phase mixture model”, *Advanced Powder Technology*. 2020;31:2480–2492. <https://doi.org/10.1016/j.apt.2020.04.012>.
11. Li Z, Yang M, Zhang Y. Lattice Boltzmann method simulation of 3-D natural convection with double MRT model. *International Journal of Heat and Mass Transfer*. 2016;94:222–238. <http://dx.doi.org/10.1016/j.ijheatmasstransfer.2015.11.042>.
12. Kolsi L, Abu-Hamdeh N, Öztop HF, Alghamdi A, Naceur BM, Ben-Assia H. Natural convection and entropy generation in a three dimensional volumetrically heated and partially divided cavity. *International Journal of Numerical Methods for Heat and Fluid Flow*. 2016;26(8):2492-2508. <https://doi.org/10.1108/HFF-09-2015-0358>.
13. Al-Rashed AAAA, Kolsi L, Hussein AK, Hassen W, Aichouni M, Borjini MN. Numerical study of three-dimensional natural convection and entropy generation in a cubical cavity with partially active vertical walls. *Case Studies in Thermal Engineering*. 2017;10:100–110. <http://dx.doi.org/10.1016/j.csite.2017.05.003>.
14. Gibanov NS, Sheremet MA. Unsteady natural convection in a cubical cavity with a triangular heat source”, *International Journal of Numerical Methods for Heat and Fluid Flow*. 2017;27:1795-1813. <https://doi.org/10.1108/HFF-06-2016-0234>.
15. Gibanov NS, Sheremet MA. Natural convection in a cubical cavity with different heat source configurations. *Thermal Science and Engineering Progress*. 2018;7:138-145. <https://doi.org/10.1016/j.tsep.2018.06.004>.
16. Gibanov N, Sheremet MA. Effect of trapezoidal heater on natural convection heat transfer and fluid flow inside a cubical cavity. *International Journal of Numerical Methods for Heat and Fluid Flow*. 2019;29 (4):1232-1248. <https://doi.org/10.1108/HFF-07-2018-0407>
17. Spizzichino A, Zemach E, Feldman Y. Oscillatory instability of a 3D natural convection flow around a tandem of cold and hot vertically aligned cylinders placed inside a cold cubic enclosure. *International Journal of Heat and Mass Transfer*. 2019;141:327–345. <https://doi.org/10.1016/j.ijheatmasstransfer.2019.06.050>.
18. Alnaqi AA, Hussein AK, Kolsi L, AL-Rashed AAAA, Li D, Ali HM. Computational study of natural convection and entropy generation in 3-D cavity with active lateral walls. *Thermal Science*. 2020;24(3B):2089-2100. <https://doi.org/10.2298/TSCI180810346A>
19. Fabregat A, Pallarès J. Heat transfer and boundary layer analyses of laminar and turbulent natural convection in a cubical cavity with differently heated opposed walls. *International Journal of Heat and Mass Transfer*. 2020;151:119409. <https://doi.org/10.1016/j.ijheatmasstransfer.2020.119409>.
20. Alshomrani AS, Sivasankaran S, Ahmed AA. Numerical study on convective flow and heat transfer in 3D inclined enclosure with hot solid body and discrete cooling. *International Journal of Numerical Methods for Heat and Fluid Flow*. 2020;30(10): 4649-4659. <https://doi.org/10.1108/HFF-09-2019-0692>.
21. Zemach E, Spizzichino A, Feldman Y. Instability characteristics of a highly separated natural convection flow: Configuration of a tandem of cold and hot horizontally oriented cylinders placed within a cold cubic enclosure. *International Journal of Thermal Sciences*. 2021;159:106606. <https://doi.org/10.1016/j.ijthermalsci.2020.106606>.
22. Hussein AK, Kolsi L, Chand R, Sivasankaran S, Nikbakhti R, Li D, Naceur BM, Aïssia HB. Three-dimensional unsteady natural convection and entropy generation in an inclined cubical trapezoidal cavity with an isothermal bottom wall. *Alexandria Engineering Journal*. 2016;55:741–755. <http://dx.doi.org/10.1016/j.aej.2016.01.004>.
23. Kolsi L, Hussein AK, Borjini MN, Mohammed HA, Ben-Aïssia H. Computational Analysis of Three-Dimensional Unsteady Natural Convection and Entropy Generation in a Cubical Enclosure Filled with Water-Al<sub>2</sub>O<sub>3</sub> Nanofluid. *Arabian Journal for Science and Engineering*. 2014; 39:7483–7493. <http://doi.org/10.1007/s13369-014-1341-y>.
24. Kolsi L, Kalidasan K, Alghamdi A, Borjini MN, Kanna PR. Natural convection and entropy generation in a cubical cavity with twin adiabatic blocks filled by aluminum oxide–water nanofluid. *Numerical Heat Transfer, Part A: Applications*. 2016; 70(3):242-259. <http://dx.doi.org/10.1080/10407782.2016.1173478>.
25. Kolsi L, Öztop HF, Alghamdi A, Abu-Hamdeh N, Borjini MN, Aïssia HB. A computational work on a three dimensional analysis of natural convection and entropy generation in nanofluid filled enclosures with triangular solid insert at the corners. *Journal of Molecular Liquids*. 2016;218:260-274. <http://dx.doi.org/10.1016/j.molliq.2016.02.083>.
26. Kolsi L, Mahian O, Öztop HF, Aich W, Borjini MN, Abu-Hamdeh N, Aïssia HB. 3D buoyancy-induced flow and entropy generation of nanofluid-filled open cavities having adiabatic diamond shaped obstacles. *Entropy*. 2016;18(6):232. <http://doi.org/10.3390/e18060232>.
27. Kolsi L, Lajnef E, Aich W, Alghamdi A, Aichouni MA, Borjini MN, Aïssia HB. Numerical investigation of combined buoyancy-thermocapillary convection and entropy generation in 3D cavity filled with Al<sub>2</sub>O<sub>3</sub>

- nanofluid. Alexandria Engineering Journal. 2016;56 (1):71-79.  
<http://dx.doi.org/10.1016/j.aej.2016.09.005>.
28. Rahimi A, Kasaeipoor A, Malekshah EH, Rashidi MM, Purusothaman A. Lattice Boltzmann simulation of 3D natural convection in a cuboid filled with KKL-model predicted nanofluid using Dual-MRT model. International Journal of Numerical Methods for Heat and Fluid Flow. 2019;9(1): 365-387.  
<https://doi.org/10.1108/HFF-07-2017-0262>.
  29. Al-Rashed AAAA, Kolsi L, Kalidasan K, Malekshah EH, Borjini MN, Kanna PR. Second law analysis of natural convection in a CNT-water nanofluid filled inclined 3D cavity with incorporated Ahmed body. International Journal of Mechanical Sciences. 2017;130:399-415.  
<http://dx.doi.org/10.1016/j.ijmecsci.2017.06.028>.
  30. Moutaouakil LE, Boukendil M, Zrikem Z, Abdelbaki A. Natural convection and thermal radiation influence on nanofluids in a cubical cavity. International Journal of Heat and Technology. 2020;38(1):59-68.  
<https://doi.org/10.18280/ijht.380107>.
  31. Sannad M, Abourida B, Belarache EH. Numerical Study of the Effect of the Nanofluids Type and The Size of the Heating Sections on Heat Transfer for Cooling Electronic Components. Journal of Advanced Research in Fluid Mechanics and Thermal Sciences. 2020;75(2):168-184.  
<https://doi.org/10.37934/arfmts.75.2.168184>.
  32. Sannad M, Abourida B, Belarache L. Numerical Simulation of the Natural Convection with Presence of the Nanofluids in Cubical Cavity. Mathematical Problems in Engineering. 2020;8375405.  
<https://doi.org/10.1155/2020/8375405>.
  33. Esfe MH, Barzegarian R, Bahiraei M. A 3D numerical study on natural convection flow of nanofluid inside a cubical cavity equipped with porous fins using two-phase mixture model. Advanced Powder Technology. 2020;31:2480-2492.  
<https://doi.org/10.1016/j.apt.2020.04.012>.
  34. Selimefendigil F, Öztop HF. Control of natural convection in a CNT-water nanofluid filled 3D cavity by using an inner T-shaped obstacle and thermoelectric cooler. International Journal of Mechanical Sciences. 2020;169:105104.  
<https://doi.org/10.1016/j.ijmecsci.2019.105104>.
  35. Al-Rashed AAAA, Kolsi L, Kalidasan K, Maatki C, Borjini M, Aichouni M, Kanna PR. Effect of magnetic field inclination on magneto-convective induced irreversibilities in a CNTwater nanofluid filled cubic cavity. Frontiers in Heat and Mass Transfer. 2017;8:31.  
<http://doi.org/10.5098/hmt.8.31>.
  36. AL-Rashed AAAA, Hassen W, Kolsi L, Oztop HF, Chamkha AJ, Hamdeh NA. Three-dimensional analysis of natural convection in nanofluid-filled parallelogrammic enclosure opened from top and heated with square heater. Journal of Central South University. 2019;26:1077-1088.  
<https://doi.org/10.1007/s11771-019-4072-0>.
  37. Bendrer BAI, Abderrahmane A, Ahmed SE, Raizah ZAS. 3D magnetic buoyancy-driven flow of hybrid nanofluids confined wavy cubic enclosures including multi-layers and heated obstacle”, International Communications in Heat and Mass Transfer. 2021; 126:105431.  
<https://doi.org/10.1016/j.icheatmasstransfer.2021.105431>.
  38. Xu X, Yu Z, Hu Y, Fan L, Cen K. A numerical study of laminar natural convective heat transfer around a horizontal cylinder inside a concentric air-filled triangular enclosure. International journal of heat and mass transfer. 2010;53(1-3):345-355.  
<https://doi.org/10.1016/j.ijheatmasstransfer.2009.09.023>.
  39. Yu ZT, Hu YC, Fan LW, Cen KF. A parametric study of Prandtl number effects on laminar natural convection heat transfer from a horizontal circular cylinder to its coaxial triangular enclosure. Numerical Heat Transfer. Part A: Applications. 2010;58(7):564-580.  
<https://doi.org/10.1080/10407782.2010.508435>.
  40. Yu ZT, Xu X, Hu YC, Fan LW, Cen KF. Unsteady natural convection heat transfer from a heated horizontal circular cylinder to its air-filled coaxial triangular enclosure. International Journal of Heat and Mass Transfer. 2011;54(7-8):1563-1571.  
<https://doi.org/10.1016/j.ijheatmasstransfer.2010.11.032>.
  41. Sourtiji E, Ganji D, Seyyedi S. Free convection heat transfer and fluid flow of Cu–water nanofluids inside a triangular–cylindrical annulus. Powder Technology. 2015;277:1-10.  
<https://doi.org/10.1016/j.powtec.2015.02.049>.
  42. Amrani AI, Dihmani N, Amraoui S, Mezrhab A. Combined natural convection and thermal radiation heat transfer in a triangular enclosure with an inner rectangular body. Defect and diffusion forum. 2018; 384:49-68.  
<https://doi.org/10.4028/www.scientific.net/DDF.384.49>.
  43. Kamiyo OM, Angeli D, Barozzi GS, Collins MW, Olunloyo VOS, Tolabi SO. A Comprehensive Review of Natural Convection in Triangular Enclosures. Applied Mechanics Reviews. 2010;63: 060801.  
<https://doi.org/10.1115/1.4004290>.
  44. Lai FH, Yang YT. Lattice Boltzmann simulation of natural convection heat transfer of Al2O3/water nanofluids in a square enclosure. International Journal of Thermal Sciences. 2011;50:1930-1941.  
<https://doi.org/10.1016/j.ijthermalsci.2011.04.015>.
  45. Oztop HF, Mobedi M, Abu-Nada E, Pop I. A heatline analysis of natural convection in a square inclined enclosure filled with a CuO nanofluid under non-uniform wall heating condition. International Journal of Heat and Mass Transfer. 2012;555076-5086.  
<https://doi.org/10.1016/j.ijheatmasstransfer.2012.05.007>.
  46. Abu-Nada E, Oztop HF. Effects of inclination angle on natural convection in enclosures filled with Cu–water nanofluid. International Journal of Heat and Fluid Flow. 2009;30(4):669-678.  
<https://doi.org/10.1016/j.ijheatfluidflow.2009.02.001>.
  47. Tric E, Labrosse G, Betrouni M. A first incursion into the 3D structure of natural convection of air in a differentially heated cubic cavity, from accurate numerical solutions. International Journal of Heat and Mass Transfer. 2000;43:4043-4056.  
[http://doi.org/10.1016/S0017-9310\(00\)00037-5](http://doi.org/10.1016/S0017-9310(00)00037-5).
  48. Peng Y, Shu C, Chew Y. A 3D incompressible thermal lattice Boltzmann model and its application to simulate natural convection in a cubic cavity. Journal of Computational Physics. 2003;193(1):260-274.  
<http://doi.org/10.1016/j.jcp.2003.08.008>.
  49. Purusothaman A, Nithyadevi N, Oztop HF, Divya V, Al-Salem K. Three dimensional numerical analysis of natural convection cooling with an array of discrete

heaters embedded in nanofluid filled enclosure. *Advanced Powder Technology*. 2016;27(1):268-280. <http://dx.doi.org/10.1016/j.apt.2015.12.012>.

---

Received 2022-03-15

Accepted 2022-05-04

Available online 2022-05-05



Prof. Dr. **Ahmed Kadhim HUSSEIN** was born in Babylon city in 19 May 1974. He gets his BSc. and MSc degrees from the University of Babylon in 1996 and 1999 respectively. He get his PhD degree from the University of Mustansriya in 2006. He awarded in 2018 the scientific excellence medal - First rank on Iraq from MHESR. He published many papers in top level journals. Now work as a professor in the University of Babylon since 2017.



**Zainab Kareem GHOBEN** was born in Diwaniyah, Iraq. She received the B.SC degree in Mechanical engineering from the University of Al-Qadisiyah. She received the M.Sc. from the University of Babylon in March 2013 and now she studying Ph.D. since September 2019 at the same university. She working at the Iraqi Agriculture Ministry and interested by the sustainable development and the 2030 SDGs, the 17 goals.